International Research Journal of Engineering and Technology (IRJET) e-ISSN: 2395-0056
Volume: 07 Issue: 10 | Oct 2020 www.irjet.net p-ISSN: 2395-0072

Study of the Structural and Elastic Properties of $Ni_{0.8}Co_{0.15}Mn_{0.05}Fe_2O_4$ Material

Negussie Tadege Demeke

Department of Mechanical Engineering, Arba Minch Institute of Technology, Arba Minch University, Arba Minch, Ethiopia

---

Abstract– $Ni_{0.8}Co_{0.15}Mn_{0.05}Fe_2O_4$ material was synthesized by sol-gel combustion method using nitrates and citric acid. The structure and elastic properties of the synthesized material were investigating using powder x-ray diffraction (XRD) and Furrier transform infrared (FTIR) spectroscopy. The structural parameters including lattice constant, unite cell volume, and crystallite size of the synthesized material were estimated. The bulk modulus, Young's modulus, rigidity modulus, longitudinal wave velocity, transverse wave velocity, and mean velocity were also evaluated from XRD and FTIR analysis values. XRD result revealed that the $Ni_{0.8}Co_{0.15}Mn_{0.05}Fe_2O_4$ material possessed a single-phase cubic spinel structure with Fd-3m space group without the presence of other phase impurities. The lattice parameter and the average crystal size of $Ni_{0.8}Co_{0.15}Mn_{0.05}Fe_2O_4$ material were also found be 0.8538 and 58.3 nm, respectively. The FT-IR analysis revealed the presence of two strong absorption bands of the tetrahedral and octahedral groups in the $Ni_{0.8}Co_{0.15}Mn_{0.05}Fe_2O_4$ material. The combined results of XRD and FTIR confirmed that the $Ni_{0.8}Co_{0.15}Mn_{0.05}Fe_2O_4$ material is mechanically stable.

Keywords: Sol-gel combustion, Structure, Elastic property, Structural parameter, cubic spinel.

1. INTRODUCTION

Ferrites are ferrimagnetic oxides consisting of ferric oxide and metal oxides. Ferrites with spinel structure belong to the important class of magnetic materials. The combination of the structural and mechanical properties makes ferrite useful in many technological applications [1]. Spinel ferrites have the general formula of MFe_2O_4, where, M usually represents one or more than one of the divalent transition metals such as Mn, Fe, Co, Ni, Cu, Zn, or other metals [2]. Other combinations of equivalent valences are also possible, such as substitution of some or all of the trivalent iron in a ferrite compound with other trivalent metal ions, such as Al^{3+}, Cr^{3+}, and Mn^{3+}ions. A unit cell of spinel ferrite material contains 32 oxygen atoms in a cubic close packing with 8 tetrahedral and 16 octahedral occupied sites [3]. Among the spinel ferrites, the inverse type is particularly interesting due to its high magneto crystalline anisotropy and unique magnetic structure [3]. $NiFe_2O_4$ is an inverse spinel ferrite in which the ferric ions are equally distributed in the tetrahedral sites and octahedral sites [4]. Some of $NiFe_2O_4$ applications are including high density magnetic recording media, magnetic refrigeration, magnetic liquids, microwave absorber and repulsive suspension for levitated railway systems [5,6]. $NiFe_2O_4$ exhibits unusual physical and chemical properties when its size is reduced in to the nanolevel. This ferrite material is prepared today by various techniques in different form and intensive research work is conducted to obtain better performing $NiFe_2O_4$ based spinel ferrite materials.

Nowadays, the synthesis of spinel ferrite nanoparticles has been intensively studied, because of their remarkable electrical and magnetic properties and wide practical application to information storage system, ferrofluid technology, magneto caloric refrigeration, catalysis, and medical diagnostics [2]. These properties are dependent on chemical composition and microstructural characteristics, which can be controlled in the fabrication and synthesis processes [2]. The principal role of the preparation conditions on the optical, electrical and microstructure features of the ferrites have been discussed in several papers; various methods of synthesizing spinel nickel ferrite nanoparticles have been reported [7]. These methods include sol-gel, hydrothermal, solid state reaction, chemical co-precipitation, molten salt etc. [7]. Among these, sol-gel combustion method is widely used for the synthesis of spinel ferrite. In this study, sol-gel combustion method was chosen for the preparation of $Ni_{0.8}Co_{0.15}Mn_{0.05}Fe_2O_4$ material. The structure and elastic properties of this material were investigated by using x-ray diffraction (XRD) and Furrier transform infrared (FTIR) spectroscopy characterization techniques.

2. MATERIALS AND METHODS

2.1. Synthesis Procedures

$Ni_{0.8}Co_{0.15}Mn_{0.05}Fe_2O_4$ material was synthesized by sol–gel combustion method. $Ni(NO_3)_2.6H_2O$, $Co(NO_3)_2.6H_2O$, $Mn(NO_3)_2.6H_2O$, $Fe(NO_3)_3.9H_2O$ and citric acid monohydrate ($C_6H_8O_7.H_2O$) were used as raw materials for the synthesis process. The stoichiometric amounts of $Ni(NO_3)_2.6H_2O$, $Co(NO_3)_2.6H_2O$, $Mn(NO_3)_2.6H_2O$, $Fe(NO_3)_3$

.9H_2O and citric acid monohydrate ($C_6H_8O_7.H_2O$) precursors was weighed out and dissolved in double distilled water and stirred for about 20 minutes. The stoichiometric amount of citric acid was dissolved in distilled water in separate beaker and stirred for about 20 minutes. The citric acid solution was further added in to the solution of nitrates. This solution was further stirred for about 15 minutes with magnetic stirrer and ammonia solution was then added under constant stirring in order to make the pH value 7. The resulting solution was continuously heated on the magnetic stirrer hotplate at 60^{0}C to form a gel. When the obtained gel is further heated at 90^{0}C, combustion process was conducted. The obtained black powder was ground in an agate mortar for about 2 hours and heated at 950^{0}c for 10 hours. Finally, this powder was ground for about using agate mortar and pestle.

2.2. Material Characterizations

X-ray powder diffraction (XRD) is one of the most valuable techniques for analyzing the following crystallographic properties: crystallite size, lattice parameter, purity, etc. of materials in powder form. It is also important to point out the unknown compounds by comparing diffraction data against a database of known powder diffraction patterns maintained by joint Committee on Powder Diffraction Standards (JCPDS). In this study, the x-ray powder diffraction pattern of $Ni_{0.8}Co_{0.15}Mn_{0.05}Fe_2O_4$ material was recorded using X-ray diffractometer (XRD-7000S diffractometer) with a Cu Kα radiation of wavelength λ = 1.5406 Å source. The measurement was conducted between a diffraction angle of 2θ = 10^o and 80^o.

Fourier transform infrared (FTIR) spectroscopy is a non-destructive characterization technique that utilizes for the identification of types of chemical bonds in the compounds by producing infrared absorption spectra. It is also used for identification of the structure of ceramic materials from the frequencies of the vibration modes. In this work, FT-IR spectroscopy measurement were accomplished using transmittance method using ALFA-T instrument with potassium Bromide (KBr) as IR window in the wave number region between 350 and 4000 cm^{-1}.

3. ESULTS AND DISCUSSION

3.1. XRD analysis

X-ray powder diffraction is a technique for analyzing the crystallite size, lattice parameter, phase identification and the unit cell volume of materials. The room temperature XRD pattern of $Ni_{0.8}Co_{0.15}Mn_{0.05}Fe_2O_4$ material prepared by using sol–gel combustion method calcined at a temperature of 950^{o}C for 10 hours is shown in Fig. 1. As it is observed from the figure, broadened, sharp and well defined XRD peaks are observed in $Ni_{0.8}Co_{0.15}Mn_{0.05}Fe_2O_4$ material. This indicates that $Ni_{0.8}Co_{0.15}Mn_{0.05}Fe_2O_4$ material possess a good crystalline structure. Most importantly, The broadening of the peaks indicates the nanocrystalline nature of synthesized material [8]. This is due to the fact that in nano sized particles there are insufficient diffraction centers, which causes the diffraction lines brooding. The XRD pattern also reveals the pure phase formation of $Ni_{0.8}Co_{0.15}Mn_{0.05}Fe_2O_4$ material without any impurity. The crystalline phase of the synthesized material is identified as a single phase cubic spinel structure with Fd-3m space group of $NiFe_2O_4$ material. Moreover, the obtained XRD peaks are also indexed using the Joint Committee on Powder Diffraction Standards (JCPDS) card with good agreement for $NiFe_2O_4$ (card no. 86-2267).

As shown in the Figure, the diffraction peaks observed at 2θ values of 30.1, 35.45, 36.87, 43.08, 53.39, 56.12, 62.48, 65.22 and 74.20^0 correspond to (111), (220), (311), (222), (400), (422), (511), (440), (620) and (533) planes, respectively. The observed peaks also confirms the formation of a spinel cubic structured in $Ni_{0.8}Co_{0.15}Mn_{0.05}Fe_2O_4$ material synthesized by sol–gel combustion method at a temperature of 950^{o}C for 10 hours using $Ni(NO_3)_2.6H_2O$, $Co(NO_3)_2.6H_2O$, $Mn(NO_3)_2.6H_2O$, $Fe(NO_3)_3.9H_2$, and $C_6H_8O_7.H_2O$ raw materials. The observed XED peaks have a very good agreement with the reported results by Yattainahalli *et al.* [9]. It is also reported that the Bragg planes of (422) and (440) correspond to tetrahedral and octahedral sites, respectively. In this study, the XRD peaks of the planes of (422) and (440) are also identified, indicating the presence of the tetrahedral and octahedral cites in $Ni_{0.8}Co_{0.15}Mn_{0.05}Fe_2O_4$ material.

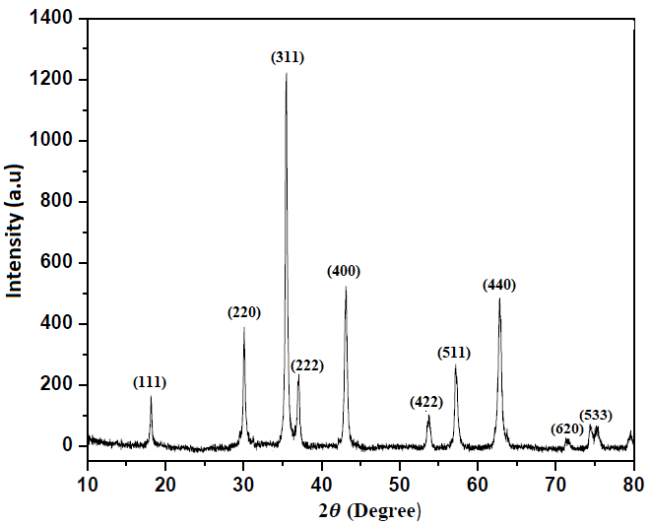

Figure-1: XRD pattern of $Ni_{0.8}Co_{0.15}Mn_{0.05}Fe_2O_4$ material.

The lattice constants (a) and the unite cell volume of $Ni_{0.8}Co_{0.15}Mn_{0.05}Fe_2O_4$ material were calculated by the least-square fitting method from the d-spacing (d) and the Miller indices (hkl) values using equations [10];

$$a = d\sqrt{h^2 + k^2 + l^2} \text{ and}$$

$$V = a^3$$

The average crystal sizes (D) of $Ni_{0.8}Co_{0.15}Mn_{0.05}Fe_2O_4$ material was also estimated by using Debye-Scherer formula [10];

$$D = \frac{0.9\lambda}{\beta \cos\theta}$$

were, λ is the wavelength of the X-ray, β is the full width at half maximum (FWHM) of the diffraction peak and θ is the Bragg's angle.

The lattice parameter is found to be 0.8344 nm for $Ni_{0.8}Co_{0.15}Mn_{0.05}Fe_2O_4$ material. Its unit cell volume is also found to be 581 $(Å)^3$.. This shows that the obtained results are slightly larger than the reported values (8.3422 Å and 581 $(Å)^3$) for the parent $NiFe_2O_4$ compound [11]. The variation in the unite cell volume and lattice constant can be explained on the basis of Vegard's law, which states that the variation in these structural parameters are related to the ionic radii of the substituted ions. In the present study, some amount of Ni^{2+} ion (ionic radius, 0.69 Å) [12] is replaced by Co^{2+} ion (ionic radius, 0.74 Å) [13] and Mn^{2+} ion (ionic radius, 0.83 Å) [13]. Thus, the substitution of Ni^{2+} ion with Co^{2+} and Mn^{2+} ions results in a slight increase in lattice constant as well as unite cell volume of $Ni_{0.8}Co_{0.15}Mn_{0.05}Fe_2O_4$ material. Similar report has been made by Babu and Tatarchuk [14]. The crystal size is found to be 61.6 nm $Ni_{0.8}Co_{0.15}Mn_{0.05}Fe_2O_4$ material, which reveals that the synthesized material the nanocrystalline nature of $Ni_{0.8}Co_{0.15}Mn_{0.05}Fe_2O_4$ material.

3.2. FTIR spectroscopic study

Fourier transform infrared spectroscopy is a common technique which is used to detect the metal-oxygen ions stretching and bending vibration in compounds. Fig. 2 shows the FTIR spectra of $Ni_{0.8}Co_{0.15}Mn_{0.05}Fe_2O_4$ material synthesized by using Sol-gel combustion method at a temperature of 950°C for 10 hours. Different researchers reported that the metal cations in $NiFe_2O_4$ material are located at tetrahedral and octahedral sites according to the geometric configuration of the oxygen ions nearest neighbors. Moreover, two main broad metal-oxygen absorption bands are found in the FTIR spectrum of $NiFe_2O_4$ material. The high frequency band υ_1 observed at around 600 cm^{-1} represent the tetrahedral metal-oxygen vibration while the low-frequency band υ_2 observed at around 400 cm^{-1} represent the octahedral metal-oxygen vibration [15]. The variation in the position of the absorption bands is due to the difference in the bond strength between the metal-oxygen coordination in the octahedral and tetrahedral sites. For instance, Srivastava et al. [10] have investigated the FTIR spectrum of $NiFe_2O_4$ material, and they reported that the absorption band v_1 around 597.94 cm^{-1} corresponds to the stretching vibrations of iron-oxygen ions band in tetrahedral sites and v_2 around 397.21 cm^{-1} is related to the stretching vibrations of iron-oxygen and nickel-oxygen bands in tetrahedral sites.

The room temperature FTIR spectrum of $Ni_{0.8}Co_{0.15}Mn_{0.05}Fe_2O_4$ material prepared by sol-gel combustion technique is shown in Fig. 2. As shown in the figure, the FT-IR analysis of $Ni_{0.8}Co_{0.15}Mn_{0.05}Fe_2O_4$ material confirms the presence of two strong absorption bands υ_1 and υ_2 which lie in the expected range of cubic spinel-type $NiFe_2O_4$ material [15]. The higher frequency band υ_1 which appears at 587 cm^{-1} is assigned to the stretching vibration of the metal-oxygen bonding force of tetrahedral group in $Ni_{0.8}Co_{0.15}Mn_{0.05}Fe_2O_4$ lattice structure [16]. While, the lower frequency band υ_2 which appears at 426.5 cm^{-1} may represent the metal-oxygen stretching vibration of octahedral group [16]. The presence of the two bands from the IR spectrum of $Ni_{0.8}Mg_{0.2}Al_{0.0\text{ -.5}}Fe_{1.95}O_4$ reveals the formation cubic spinel nano material. Different researchers have identified that the normal mode of vibration of the tetrahedral cluster is higher than that of the octahedral cluster. This change is related to the shorter bond length of the tetrahedral cluster and the longer bond length of the octahedral cluster [12]. As compared with the bands of $NiFe_2O_4$ compound reported by Srivastava et al. [10], the absorption peak of in the $Ni_{0.8}Co_{0.15}Mn_{0.05}Fe_2O_4$ lattice is shifted towards lower wavenumber region, which is in good agreement with the lower lattice parameter, unit cell volume and crystal size calculated from the XRD pattern.

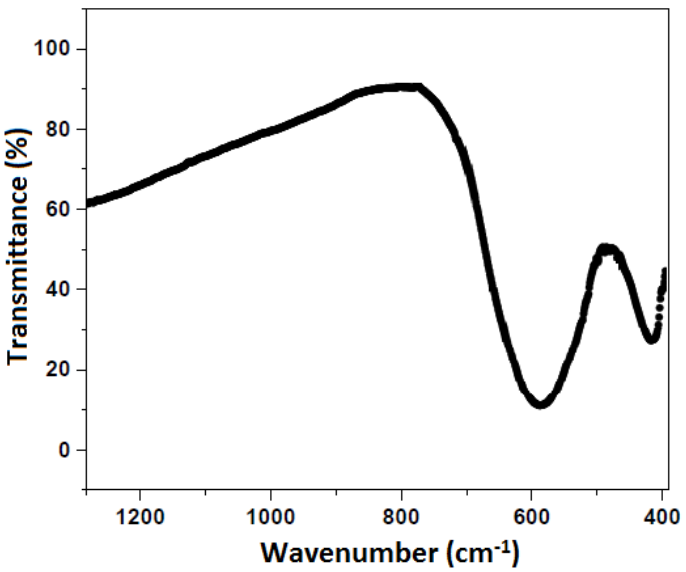

Figure-2: FTIR spectrum of $Ni_{0.8}Co_{0.15}Mn_{0.05}Fe_2O_4$ material.

The value of the force constants for tetrahedral sites K_T and octahedral sites K_O were calculated by using the following relation;

$$K_t = 7.62 \times M_1 \times v_1^2 \times 10^{-7}\ N/m$$

$$K_o = 10.62 \times \frac{M_2}{2} \times v_2^2 \times 10^{-7}\ N/m$$

where M_1 is the molecular weight of cations at the tetrahedral site, M_2 is the molecular weight of cations at the octahedral site, v_1 is the frequency band at tetrahedral site and v_2 is also the frequency band at the octahedral site. The elastic force constants for tetrahedral (K_t) and octahedral site (K_O) for $Ni_{0.8}Co_{0.15}Mn_{0.05}Fe_2O_4$ material are found to be 1.5×10^5 dyne/cm and 1.1×10^5 dyne/cm. This confirms that the elastic force constant of K_t is larger than that of K_o, which is associated with the shorter bond length of the tetrahedral cluster and longer bond length of octahedral cluster in $Ni_{0.8}Co_{0.15}Mn_{0.05}Fe_2O_4$ material. It knows that bond length and the force constants have an inverse proportionality [17].

3.3. Elastic properties

The elastic properties study of solid materials are important for investigating the strength of binding forces in materials. Elastic properties of the ferrite materials can be estimated from the obtained XRD and FT-IR analysis. The stiffness constants C_{11} and C_{12} of $Ni_{0.8}Co_{0.15}Mn_{0.05}Fe_2O_4$ material were calculated using the relations [16] :

$$C_{11} = \frac{K_T + K_O}{2a}$$

$$C_{12} = \frac{C_{11}}{(1-\sigma)}$$

where 'a' is lattice constant and σ is the poisons ratio. The elastic moduli of $Ni_{0.8}Co_{0.15}Mn_{0.05}Fe_2O_4$ material were also calculated using the following relations [18,19]:

$$B = \frac{1}{3}(C_{11} + 2C_{12})$$

$$Y = \frac{(C_{11}-C_{12})+(C_{11}+2C_{12})}{C_{11}+C_{12}}$$

$$G = \frac{Y}{2(1+\sigma)}$$

where B is bulk modulus, Y is Young's modulus and G is rigidity modulus. The longitudinal wave velocity V_L, the transverse wave velocity V_s and the mean velocity V_m of $Ni_{0.8}Co_{0.15}Mn_{0.05}Fe_2O_4$ material were also evaluated using the relations [18,20];

$$V_L = \left(\frac{C_{11}}{D_b}\right)^{1/2}$$

$$V_s = \frac{V_L}{\sqrt{3}}$$

$$V_m = \left[\frac{1}{3}\left(\frac{2}{V_s^3} + \frac{1}{V_L^3}\right)\right]^{-1/3}$$

where D_b is the bulk density. The poisons ratio σ of the material was also calculated using the relation [20];

$$\sigma = \frac{V_L^2 - 2V_s^2}{2(V_L^2 - V_s^2)}$$

The Debye temperature θ_D is a fundamental attribute of solid connecting elastic properties with thermodynamic properties such as specific heat. The Debye temperature of $Ni_{0.8}Co_{0.15}Mn_{0.05}Fe_2O_4$ material was calculated by using the relation [18];

$$\theta_D = \frac{hV_m}{k}\left[\left(\frac{3\rho q N_A}{4\pi M}\right)\right]^{1/3}$$

where h is Planck constant (6.626×10^{-34} Js) , k is Boltzmann constant (1.38×10^{-23} J/K), N_A is Avogadro's number (6.022×10^{23} 1/mol), M is molecular weight of the sample, q is number of atoms in the unit formula, ρ is the density of the sample. The values of C_{11} and C_{12} are found to be 156 GPa and 53.4 GPa, respectively. This indicates that C_{11} is significantly larger than that of C_{12}. It is also observed that the calculated C_{11} and C_{12} are positive and satisfied the mechanical stability condition in a cubic crystal, which is $(C_{11} - C_{12}) > 0$, $(C_{11}+2C_{12}) > 0$, $C_{11} > 0$ and $C_{12} < B < C_{11}$.This suggests that both the synthesized $Ni_{0.8}Co_{0.15}Mn_{0.05}Fe_2O_4$ material is mechanically stable [21].

The calculated values of the bulk modulus (B), Young's modulus (Y), and rigidity modulus (G) of $Ni_{0.8}Co_{0.15}Mn_{0.05}Fe_2O_4$ material are found to be 87.6, 1.75, and 69.7 GPa, respectively. The longitudinal wave velocity (V_L) of $Ni_{0.8}Co_{0.15}Mn_{0.05}Fe_2O_4$ material is also found to be 6261 m/s, which is higher than the value of the shear wave velocity (Vs), 3614.8 m/s. According to a previous report [16], when a wave travels through a material, it makes the particles vibrate. The vibrating particles collide with neighboring particles, which results in other particles to vibrate and longitudinal and shear elastic waves are produced. The particles in a material vibrates perpendicular to the direction of propagation of wave motion during the shear wave, and hence it requires a larger energy to make the neighboring particle vibrate. This, in turn, results in decrease in energy of wave velocity, and hence the shear wave velocity is nearly one-half of its longitudinal wave velocity [16].

The value of Poisson's ratio is found to be 0.24 for $Ni_{0.8}Co_{0.15}Mn_{0.05}Fe_2O_4$ material. The obtained values lie in the range between -1 and 0.5, which is in conformity with theory of isotropic elasticity. The Debye temperature is an important parameter, which helps to understand the variations in thermodynamic properties such as the maximum atomic displacement, specific heat, melting temperature, or vibrational entropy [16]. It is the temperature at which the maximum lattice vibrations take place. In this study, the Debye temperature $Ni_{0.8}Co_{0.15}Mn_{0.05}Fe_2O_4$ material is found to be 384.3 K.

4. CONCLUSIONS

$Ni_{0.8}Co_{0.15}Mn_{0.05}Fe_2O_4$ material was successfully synthesized by sol-gel combustion method using citric acid as a fuel and chelating agent. The XRD study confirmed the formation of a cubic spinel-type $Ni_{0.8}Co_{0.15}Mn_{0.05}Fe_2O_4$ material with lattice parameters and an average crystallite size of 0.8344 nm and 61.6 nm, respectively. The room temperature FTIR spectroscopic study of $Ni_{0.8}Co_{0.15}Mn_{0.05}Fe_2O_4$ material confirmed the formation of two strong absorption bands. The higher frequency band which appeared at 587 cm^{-1} assigned to the stretching vibration of the metal-oxygen bonding force of tetrahedral. The lower frequency band that appeared at 426.5 cm^{-1} represented the metal-oxygen stretching vibration of octahedral group. The combined results of XRD and FTIR confirmed that the substitution of Co^{2+} and Mn^{2+} for Ni^{2+} did not change the basic structure of the spinel $NiFe_2O_4$ material. The calculated force constants of the tetrahedral site K_T and octahedral site K_o, elastic constants, electric moduli, elastic velocities and Debye temperature were also matched with the reported values for $NiFe_2O_4$ material. From the elastic property study, it was identified that the synthesized $Ni_{0.8}Co_{0.15}Mn_{0.05}Fe_2O_4$ material is mechanically stable.

ACKNOWLEDGEMENT

The author gratefully acknowledges Dr. Paulos Taddesse for his support. The author also acknowledges Dr. Vijaya Babu, Andhra University, for conducting XRD, FTIR and SEM characterization.

REFERENCES

[1] B.T. Chiad and R. A. Mohammed, Structural properties of magnetic measurement of nanostructure $NiFe_2O_4$ prepared by Co-sputtering technique, international journal of new technology and research, vv. 3, 2017, pp. 56-58.

[2] V.D. Murumkar, Effect of zinc substitution on magnetic properties of nickel ferrite nanoparticles, International journal of education and applied science research, vv.3, 2016, pp. 41-48.

[3] C. Yao, Z. Yuanhui, W. Yuansheng, B. Feng and Q. Yong, Synthesis and magnetic properties of nickel ferrite nano – octahedral, journals of solid state chemistry, vv. 178, 2005, pp. 2394-2397.

[4] M.V. Kovalenko, M.I. Bodnarchuk, R.T. Lechner, G. Hesser, F. Schaffler, W. Hess, Fatty acid salts as stabilizers in size and shape controlled nanocrtstal synthesis, The case of inverse spinel iron oxide, Journal of the American Chemical society, vv. 129, 2007, pp. 6352-6353.

[5] C.G. Remankutty, S. Sugunan, Surface properties and catalytic activity of ferro spinels of nickel, cobalt and copper prepared by soft chemical methods, Applied catalysis A General, vv. 218, 2001, pp. 39-51.

[6] T. Tetiana, B. Mohamed, J.J. Vijaya, L.J. Kennedy, Spinel ferrite nanoparticles: synthesis, crystal structure properties, and perspective application, Springer international publishing, vv. 8, 2017, pp. 305.

[7] J. Tan, W. Zhang, A. Xia, Facile Synthesis of inverse spinel $NiFe_2O_4$ nanocrystals and their superparamagnetic properties. Materials Research, vv. 16, 2013, pp. 237-241.

[8] S. Kumar, A. Sharma, M. Singh and S. P. Sharma, Simple synthesis and magnetic properties of nickel-zinc ferrites nanoparticles by using aloe vera extract solution Archive of applied science research, vv. 5, 2013, pp. 145-151.

[9] S.S. Yattinahalli, S.B. Kapatkarr, S.N. Mathad, Structural and mechanical properties of nano ferrite, advanced science focus, vv. 2, 2014, pp. 42-46.

[10] M. Srivastava, A.K. Ojha, S. Chaubey, A. Materny, Synthesis and optical characterization of nanocrystalline NiFe2O4 structures, Journal of Alloys and Compounds, vv. 481, 2009, pp. 515–519.

[11] A. Gaffoor, D. Ravinder, Characterization of magnesium substituted Nickel Nano ferrites synthesized By Citrate-Gel Auto Combustion Method, Journal of Engineering Research and Applications:, vv. 4, 2014, pp. 60-66.

[12] D. Varshney, Kavita Verma, Substitutional effect on structural and dielectric properties of $Ni_{x-1}A_xFe_2O_4$ (A = Mg, Zn) mixed spinel ferrites, Materials Chemistry and Physics, vv. 140, 2013, pp. 412-418.

[13] A.D.Fortes, I.G. Wood, K.A. Hudson-dwards, M.J. Gutmanna, Partitioning of Co^{2+} and Mn^{2+} into meridianiite ($MgSO_4{\cdot}11H_2O$): Ternary solubility diagrams at 270 K; cation site distribution determined by single-crystal time-of-flight neutron diffraction and density functional theory, Fluid Phase Equilibria, vv. 437, 2017, pp. 1-13.

[14] B.R. Babu, T. Tatarchuk, Elastic properties and antistructural modeling for Nickel-Zinc ferrite-aluminates, Materials Chemistry and Physics, vv. 207, 2018, pp. 534-541.

[15] B. Senthilkumar, R. KalaiSelvan, P. Vinothbabu, I. Perelshtein, A. Gedanken, Structural, magnetic, electrical and electrochemical properties of $NiFe_2O_4$ synthesized by the molten salt technique, Materials Chemistry and Physics, vv. 130, 2011, pp. 285–292.

[16] B.R. Babu, T. Tatarchuk, Elastic properties and antistructural modeling for Nickel-Zinc ferrite-aluminates, Materials Chemistry and Physics, vv. 207, 2018, pp. 534-541.

[17] S. C.Watawe, B. D. Sutar, B. D. Sarwade, and B. K. Chougule, (2001). Infrared studies of some mixed Li-Co ferrites, International journal of inorganic materials, vv. 3, 2001, pp. 819–823.

[18] K.B. Modi, M.C. Chhantbar, P.U. Sharma, H.H. Joshi, Elastic constants determination for Fe^{3+} substituted

YIG through infra-red spectroscopy and heterogeneous metal mixture rule, Journal of materials science, vv. 40, 2005, pp. 1247 – 1249.

[19] J.D. Baraliya, H.H. Joshi, Spectroscopic and thermographic study of Ni–Zn ferrites, Journal of Thermal Analysis and Calorimetry, vv. 119, 2015, pp. 85–90.

[20] A. Bhaskar, S.R. Murthy, Effect of sintering temperatures on the elastic properties of Mn (1%) added MgCuZn ferrites, Journal of Magnetism and Magnetic Materials, vv. 355, 2014, pp. 100-103

[21] J. Wang, S. Yip, Crystal instabilities at finite strain, Physics Review letter, vv. 71, 1993, pp. 4182.